Determination of Oil Palm Planting Patterns using ArduSimple RTK2B GNSS, LoRa Communication, and Drone-based Orthophotos

Mona Arif Muda Batubara*, Muna Fauziah, Melvi & Ardian Ulvan

Department of Electrical Engineering, Universitas Lampung, Jalan Sumantri Brojonegoro No.1, Bandar Lampung 35145, Lampung, Indonesia
*E-mail: mona.batubara@eng.unila.ac.id

Abstract. Oil palm is a major plantation commodity in Indonesia, where accurate planting patterns are essential to optimize yield and support sustainable management. Conventional methods using stakes and ropes are labor-intensive and prone to spatial error, whereas many GNSS-based systems are costly and proprietary. This study develops a low-cost real-time kinematic (RTK) GNSS system for determining oil palm planting patterns, based on the ArduSimple RTK2B module, a multiband GNSS antenna, and long-range LoRa communication integrated with a mobile application and orthophoto-derived digital maps. In the base–rover configuration, RTCM corrections are transmitted via LoRa, while planting points designed in ArcGIS are imported into SW Maps for field navigation. Performance is assessed through benchmark accuracy tests, LoRa packet delivery ratio and packet loss measurements over 10–100 m, planting-pattern trials for square and triangular layouts, and a comparison with an actual oil palm layout in a commercial estate. The rover achieved a horizontal positioning error of 8.95 cm, while planting trials yielded mean errors of 8.40 cm (RMSE 9.3 cm) for the square layout and 7.78 cm (RMSE 9.1 cm) for the triangular layout, both within the 10 cm tolerance. The proposed system provides practical, low-cost accuracy for oil palm planting guidance.

Keywords: *ArduSimple RTK2B; LoRa; oil palm planting pattern; orthophoto; RTK GNSS.*

1 Introduction

Oil palm (Elaeis guineensis) is one of Indonesia's most important plantation commodities and a major contributor to national export income. Favorable tropical climatic conditions and fertile soils have enabled rapid expansion of oil palm plantations. By 2018 the planted area reached 14.3 million hectares, with a national production of 37.5 million tonnes, comprising 31.3 million tonnes of crude palm oil (CPO) and 6.2 million tonnes of palm kernel oil [1]. Riau Province is the largest producer, with 2.86 million hectares of oil palm plantations and an output of 8.86 million tonnes [1].

The planting pattern is one of the most critical factors in oil palm cultivation, because it determines tree density, spatial distribution, and long-term

Received December 8th, 2025, Revised June 11th, 2026, Accepted for publication June 17th, 2026.
 ISSN: 2337-5787, DOI: 10.5614/itbj.ict.res.appl.2026.20.2.4

productivity. Appropriate spacing maximizes land use, reduces inter-tree competition for light, water, and nutrients, and facilitates access for maintenance and harvesting. Latifian, *et al.* [2] reported that improving the number of productive trees per hectare can increase cumulative yield by around 1% under various environmental conditions. Consequently, accurate and repeatable positioning of planting points is essential to ensure efficient and sustainable plantation management [3].

In practice, however, planting points in many estates are still established using conventional methods such as stakes, ropes, and manual tape measurements. These procedures are labor-intensive, time-consuming, and highly dependent on operator skill, making them prone to spatial inaccuracies, especially over large blocks or undulating terrain. While high-end GNSS-based solutions and automatic planters have been introduced by several manufacturers and previous studies, their high cost, proprietary nature, and limited flexibility make them less accessible for smallholder plantations and medium-scale estates.

To address these limitations, this study develops and evaluates an integrated, low-cost planting pattern determination system based on real-time kinematic (RTK) GNSS, LoRa communication, and orthophoto-derived digital maps. The system uses an ArduSimple RTK2B module with a multiband GNSS antenna configured in a base–rover architecture, where RTCM correction data are transmitted via LoRa to a rover unit that guides operators to each planting point using the SW Maps smartphone application. Planting patterns are generated in ArcGIS on top of orthophotos and then imported to the rover for field navigation. The main contributions of this work are: (i) the design of an open, low-cost RTK GNSS–LoRa system tailored for oil palm planting applications; (ii) experimental evaluation of its positional accuracy and communication performance under realistic field conditions; and (iii) validation of the designed planting patterns through field trials and comparison with an existing commercial plantation layout.

2 Related Works

Several studies have examined the application of GNSS RTK for high-accuracy land measurement and guidance in agricultural operations. Gumilar [4] analyzed the accuracy of land-parcel measurements using RTK GNSS and reported that the method provides centimeter-level positional precision with low measurement error, making it suitable for cadastral and boundary surveys. In the context of oil palm, Nur Aini *et al.* [5] developed an automatic planting-point marking system using JAVAD GNSS equipment to generate layout coordinates for plantation establishment. These works demonstrate the potential of RTK GNSS for precise spatial positioning, but they typically rely on high-end, proprietary receivers.

Building on this foundation, the present study employs an ArduSimple RTK2B module integrated with a multiband GNSS antenna to offer a more cost-effective, open, and flexible solution while targeting comparable positioning performance.

The planting pattern of oil palm has a direct impact on plantation productivity, as optimal spacing maximizes land utilization and minimizes inter-tree competition for sunlight, nutrients, and water. James and Jayaselan [6], in their study "Development of a Mechanization Selection System for Oil Palm Plantations with Alternative Planting Patterns," identified four major planting patterns: square, triangular, rectangular, and hexagonal. Each configuration offers distinct advantages depending on terrain characteristics, topography, and operational efficiency in plantation management.

Orthophoto technology plays a crucial role in precision agriculture, providing geospatial data that support accurate plantation analysis and planning. As a type of photographic map, an orthophoto provides spatial accuracy comparable to conventional topographic maps and serves as an essential component in photogrammetry [7]. The study "Interpretation of UAV Orthophoto Geospatial Data for Oil Palm Land Monitoring" [8] demonstrated the potential of UAV-based orthophoto mapping to enhance land-monitoring accuracy, reduce field errors, and improve plantation-management efficiency.

More recently, the positioning performance of compact, low-cost GNSS modules in RTK mode has been studied in detail. Mahato *et al.* [9] evaluated several compact, low-cost GNSS receiver–antenna combinations and reported RTK accuracies competitive with geodetic-grade equipment under open-sky conditions, while the same group demonstrated single-baseline long-distance RTK using a compact module and open-source software [10] and characterized the position-solution quality of low-cost dual-frequency modules [11]. These results confirmed that multi-band consumer-grade receivers can sustain centimeter-level fixes. Performance in obstructed environments has also been assessed; RTK quality under forest canopy was shown to degrade with increasing multipath and signal blockage [12], a finding directly relevant to mature oil palm stands. In the photogrammetric domain, Famiglietti *et al.* [13] integrated a low-cost RTK/PPK GNSS module on a UAV and achieved a vertical RMSE below 2 cm for the resulting digital elevation models, illustrating the synergy between low-cost RTK positioning and orthophoto-based mapping. Collectively, these works establish the feasibility of low-cost RTK; however, most focused on positioning accuracy alone and rely on internet-based (NTRIP) or UHF correction links. Few integrated an autonomous LoRa-based RTCM transport with orthophoto-derived planting design for direct field guidance in plantation establishment, which is the gap addressed by the present study.

3 System Overview and Base Station Configuration

This study developed an integrated device and workflow for visualizing oil palm planting patterns and guiding their field implementation. The system adopts a base–rover architecture in which planting points are first designed in a geographic information system (GIS) environment and then transferred to a mobile platform for on-site navigation. Orthophoto imagery of the plantation area is used to delineate block boundaries and generate a regular grid of planting points in ArcGIS. The overall data flow of the system, from base-station correction generation, through LoRa transport, to rover positioning and smartphone-based navigation, is summarized in Figure 1.

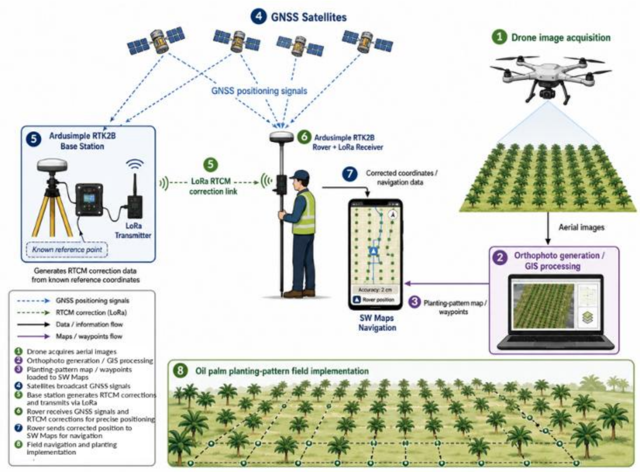

Figure 1 System architecture of the integrated RTK GNSS–LoRa–orthophoto planting-pattern system, showing the base station, LoRa RTCM link, rover, and SW Maps navigation flow. (Note: picture was generated by AI; www.chatgpt.com).

The design rationale is as follows. The base–rover architecture was selected in preference to network RTK (NTRIP), because oil palm blocks are frequently located in areas with limited or no cellular coverage; a self-contained local base removes any dependence on internet connectivity and keeps the baseline short, which is favorable for rapid ambiguity resolution and reliable fixes. LoRa was chosen as the correction-transport layer for its long range, low power consumption, and license-free operation, making it well suited to plantation environments where wired links are impractical and cellular data is unreliable. The ArduSimple RTK2B (based on the u-blox ZED-F9P) was adopted because it is an open, multi-constellation, multi-band receiver that delivers dual-frequency measurements at low cost, mitigating ionospheric error and shortening time-tofix relative to single-band modules. Finally, operating the base in survey-in mode until convergence and then switching to fixed-coordinate mode provides a stable, repeatable reference, which is essential for consistent centimeter-level rover corrections across repeated field sessions.

The resulting coordinates are exported and imported into the SW Maps application, which runs on an Android smartphone connected to the rover unit. The base station acts as a fixed reference that broadcasts RTK correction messages, while the rover receives these corrections in real time to compute high-accuracy positions and display each target planting point on the smartphone screen, thus eliminating the need for manual tape measurements and physical markers. The base station was configured using the ArduSimple RTK2B module and u-blox u-center v.22 software, following the steps summarized in Table 1, which include setting the reference position, enabling RTK message types, defining the update rate, and configuring serial ports for data output to the Raspberry Pi 4.

Table 1 ArduSimple RTK2B base configuration in u-center v.22.

Step	Configuration Step	Notes
Connect GNSS to PC	Connect GNSS module to the PC with Micro-USB to USB cable	Verify if the driver is installed
Open u-center v.22	Open u-center v.22 and select the appropriate COM port	Confirm the port in Device Manager
Adjust baud rate	In the Receiver menu, select baud rate	Set it to 115200
Check the connection	View → Message → UBX-NAV-PVT	Data should appear
Set communication port	UBX → CFG → PRT and configure the port	Match the port used
Activate base mode	UBX → CFG → TMODE3 and select Survey-In	Set duration and minimum accuracy
Use fixed coordinates	After convergence, switch to Fixed mode	Improves rover correction accuracy
Set rover operating mode	UBX → CFG → NAV5 → Dynamic Model: Pedestrian	For walking-speed rover use
Confirm fixed base	After obtaining the coordinates, ensure TMODE3 is set to Fixed mode	Stabilizes the reference
Save configuration	UBX → CFG → CFG → Save current configuration → Send	Prevents the configuration from resetting

The ArduSimple RTK2B module was interfaced with a Raspberry Pi 4 via USB for configuration, data logging, and management of the correction streams. External multiband GNSS antennas were installed at both the base and the rover to ensure robust satellite reception, while LoRa Ebyte E220 transceivers transmitted the RTCM correction data from the base to the rover. The rover module was paired with an Android smartphone via Bluetooth, allowing NMEA position data to be received by SW Maps in real time. Power was supplied from a portable DC source and the overall hardware arrangement was designed to be compact and easily deployable in plantation environments. A detailed list of the components and software is provided in Table 2.

Table 2 Components and software used in the device.

Component / Software	Description of Use
ArduSimple RTK2B	GNSS receiver operating at both the base station and the rover
GNSS Multiband Antenna (IP66)	Rover antenna
GNSS Multiband Antenna (IP67)	Base antenna
u-blox u-center v.22	Configuration software
Raspberry Pi 4 Model B	Microcomputer integrating the system
LoRa Ebyte E220-900T22D	Radio module for rover–base communication
Buck-boost converter	Voltage-adjustment module
Battery 12 V 7 Ah (Panasonic)	Power supply
SW Maps	Software for displaying the system data
Google Earth Pro	Observation, orthophoto overlay, and visualization of the ArcGIS pattern
ArcGIS	Generation of the planting pattern

Determination of the planting-pattern points began with extracting the boundary of the study block from Google Earth and importing it into ArcGIS. Within this boundary, a fishnet grid was generated according to the desired planting distance for the square and triangular configurations. Grid-intersection points representing tree locations were then converted into point features and attributed with unique identifiers. The final set of planting points was exported as KML and GeoJSON files for two purposes: visualization and verification in Google Earth and importing into SW Maps as the user-interface layer for field navigation. This process ensured geometric consistency between the digital design and the coordinates used by the rover in the field. The default device GPS was then configured to act as a GNSS receiver within SW Maps, enabling real-time display of both the planting pattern and the user location, as illustrated in Figure 2 for the case of a demonstration conducted at the Universitas Lampung field.

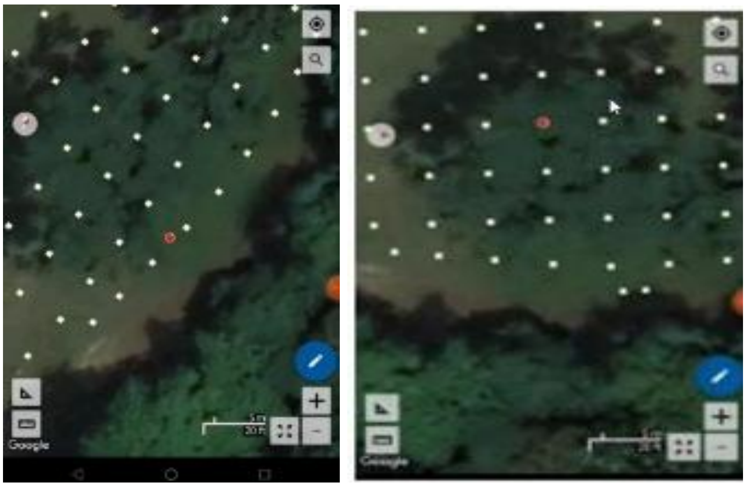

Figure 2 Visualization of the planting pattern and user location in SW Maps during the demonstration at the Universitas Lampung field.

4 Results and Discussion

4.1 GNSS Positioning Accuracy

The system-testing phase evaluated both the GNSS accuracy and the LoRa communication performance. The GNSS accuracy test compared the rover's measured coordinates against a benchmark point located near the Universitas Lampung Library, whose coordinates had previously been determined using static GNSS survey methods [14].

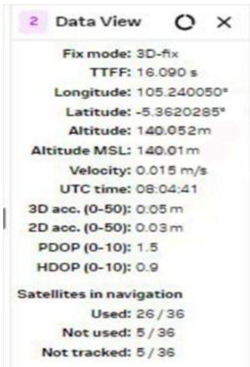

Figure 3 RTK Fixed (3D Fixed) status of the rover displayed in the u-center data view.

The test verified that the rover achieved the required precision level (error < 10 cm). Both the base and rover modules were activated, the rover's coordinates were recorded once it reached RTK Fixed / 3D Fixed status, and data were collected after this state had been maintained for five minutes [14]. Figure 3 shows the RTK Fixed status of the rover in the u-center data view.

During testing, the rover maintained a 3D Fixed / RTK Fixed solution and recorded a latitude of −5.3620285° S and a longitude of 105.2400516° E, while the benchmark coordinates were −5.3620278° S and 105.2400520° E. Using standard geodetic approximations (1° of latitude ≈ 111.32 km and 1° of longitude ≈ 110.83 km at the study latitude), the latitude and longitude differences correspond to horizontal offsets of approximately 7.8 cm and 4.4 cm, respectively. The resulting horizontal positional error, obtained from the Pythagorean combination of the two components, was about 8.95 cm, which satisfies the < 10 cm accuracy requirement for precise planting-point marking.

4.2 LoRa Communication Performance

LoRa communication performance was assessed by measuring the packet delivery ratio (PDR) and packet loss (PL) between the base and the rover at separation distances of 10, 20, 30, 40, 50, 60, 70, 80, 90, and 100 m. At each distance, RTCM correction messages were transmitted continuously for 60 s and the numbers of packets sent and received were recorded [15]. PDR (%) was computed as the ratio of received to transmitted packets, while PL (%) was calculated as 100 − PDR. The results, summarized in Table 3 and illustrated in Figures 4 and 5, show that communication performance remained high at short ranges but degraded gradually with distance, with a marked decrease in PDR and a corresponding increase in PL beyond 90 m, indicating reduced reliability of the correction link at longer ranges.

Table 3 LoRa performance over a 60-second transmission window.

Distance (m)	Packets Sent (Base)	Packets Received (Rover)	PDR (%)	Packet Loss (%)
10	25	25	100.00	0.00
20	26	25	96.15	3.85
30	25	24	96.00	4.00
40	24	23	95.83	4.17
50	25	23	92.00	8.00
60	25	22	88.00	12.00
70	23	20	86.96	13.04
80	24	20	83.33	16.67
90	24	19	79.17	20.83
100	23	18	78.26	21.74

Figure 4 Packet delivery ratio (PDR, %) versus base–rover distance (m).

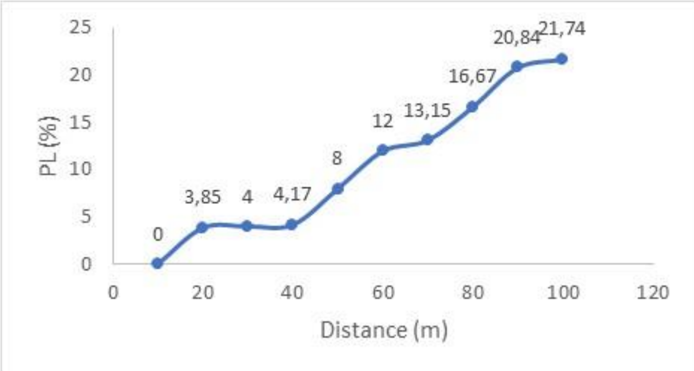

Figure 5 Packet loss (PL, %) versus base–rover distance (m).

4.3 Planting-Pattern Field Trials

Following validation of the communication link, field trials examined the effectiveness of the system in guiding the implementation of oil palm planting patterns. The first set of trials applied a square planting pattern across three areas located at increasing distances from the base station. In each area, a series of target points was navigated using the rover and SW Maps and the actual distances between planted points were measured and compared with the design spacing. The second set of trials employed a triangular planting pattern over a similar arrangement of areas. The spatial distribution of the measured points for both patterns is shown in Figure 6 and the detailed numerical results are provided in Tables 4 and 5.

To quantify the reliability of the planting-pattern implementation, descriptive statistics were computed for the per-point spacing errors of both layouts (Table 6). For the square pattern ($n = 15$), the mean error was 8.40 cm, with a standard deviation of 4.08 cm, a root-mean-square error (RMSE) of 9.28 cm, and a 95% confidence interval for the mean of 6.14–10.66 cm; errors ranged from 1 to 15 cm. For the triangular pattern ($n = 18$), the mean error was 7.78 cm with a standard deviation of 4.82 cm, an RMSE of 9.08 cm, and a 95% confidence interval of

5.38 to 10.18 cm; errors ranged from 2 to 17 cm. In both layouts the mean and the RMSE remained below the 10 cm tolerance required for planting-point marking, confirming that the system delivers practically adequate accuracy. Importantly, the largest individual errors (15 cm and 17 cm) occurred exclusively in the areas farthest from the base station and the moderate standard deviations (about 4–5 cm) were driven mainly by these far-area points rather than by any systematic bias near the base.

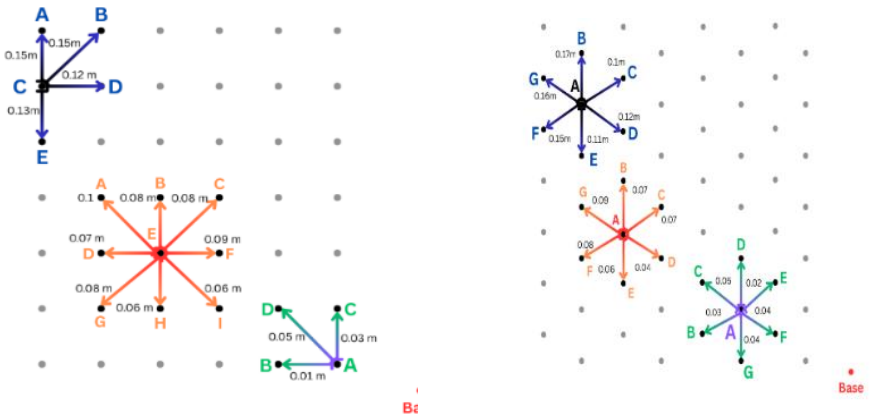

Figure 6 Spatial distribution of the measured points for the square and triangular planting patterns.

Table 4 Measurement data for a square pattern.

Area	Point	Planned Distance (m)	Measured Distance (m)	Error (cm)
1	A–B	8	8.01	1
1	A–C	8	8.03	3
1	A–D	11.30	11.35	5
2	C–A	8	8.15	15
2	C–E	8	8.13	13
2	B–C	11.30	11.45	15
2	C–D	8	8.12	12
3	E–A	11.30	11.40	10
3	E–B	8	8.08	8
3	E–C	11.30	11.38	8
3	E–D	8	8.07	7
3	E–F	8	8.09	9
3	E–G	11.30	11.38	8
3	E–H	8	8.06	6
3	E–I	11.30	11.36	6

Table 5 Measurement data of points in a triangular pattern.

Area	Point	Planned Distance (m)	Measured Distance (m)	Error (cm)
1	A–B	8	8.03	3
1	A–C	8	8.05	5
1	A–D	6.9	6.92	2
1	A–E	8	8.02	2
1	A–F	8	8.04	4
1	A–G	6.9	6.94	4
2	A–B	6.9	6.97	7
2	A–C	8	8.07	7
2	A–D	8	8.04	4
2	A–E	6.9	6.94	4
2	A–F	8	8.08	8
2	A–G	8	8.09	9
3	A–B	6.9	7.07	17
3	A–C	8	8.10	10
3	A–D	8	8.12	12
3	A–E	6.9	7.01	11
3	A–F	8	8.15	15
3	A–G	8	8.16	16

Table 6 Summary statistics of the per-point spacing errors (cm).

Statistic	Square (n = 15)	Triangular (n = 18)
Mean error	8.40	7.78
Standard deviation	4.08	4.82
RMSE	9.28	9.08
Minimum	1	2
Maximum	15	17
Range	14	15
95% confidence interval (mean)	6.14–10.66	5.38–10.18

This behavior shows that as the distance from the base increases, the mean error tends to rise, indicating that base–rover separation has a significant influence on measurement accuracy. Figure 7 illustrates the mode and lowest error values (in cm) for each area in the square and triangular patterns. The mode of the error in each area increases with distance from the base, which aligns quantitatively with the LoRa communication test: as the base–rover distance grows, PDR decreases and PL increases, so a portion of the RTCM corrections is not received by the rover, resulting in larger positional errors. The mode-error data therefore consistently demonstrate a decline in positional accuracy in areas located farther from the base.

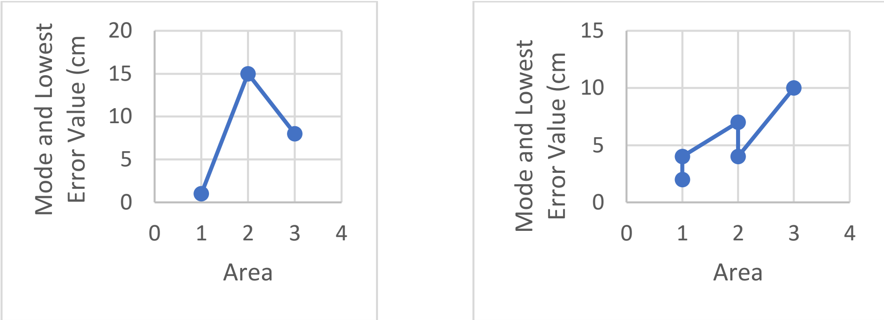

Figure 7 Mode and lowest spacing-error values (cm) per area for the square and triangular planting patterns.

4.4 Comparison with an Existing Plantation Layout

A fourth test evaluated how well the digitally designed planting pattern matched an existing oil palm plantation layout. The planting points generated in ArcGIS were overlaid on Google Earth orthophoto imagery covering a block of PT Bina Sawit Makmur (BSM) Sampoerna Agro, Mesuji (Figure 8). The overlay allowed assessment of the correspondence between the planned tree locations and the actual tree positions visible in the orthophoto.

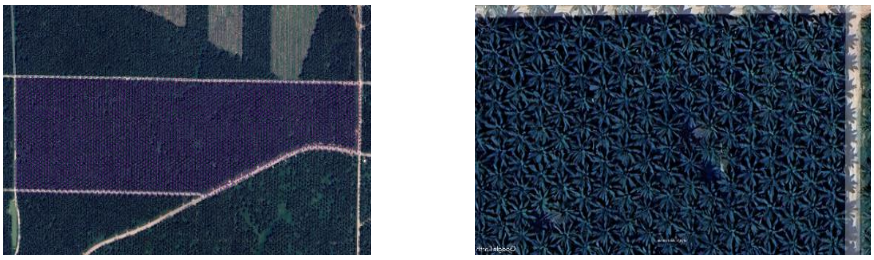

(a) (b)

Figure 8 Overlay of the designed planting pattern on the Google Earth orthophoto of PT Bina Sawit Makmur (BSM): (a) designed grid; (b) actual plantation.

The overlay reveals a consistent positional shift between the designed points and the observed tree crowns in several parts of the block. Examination of elevation profiles along selected transects (Figure 9) indicated that the best alignment occurred at elevations between 23 and 24 m, suggesting that local topography influenced how the planting lines were realized in the field.

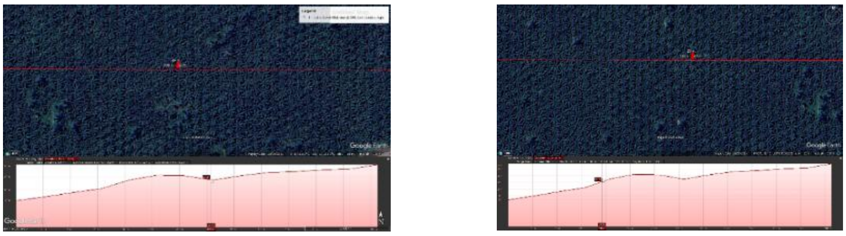

(a) (b)

Figure 9 Elevation profile along the evaluated transects at PT Bina Sawit Makmur (BSM): (a) and (b) selected transects.

The overall correspondence between the digital design and the actual configuration in the field, estimated at approximately ±25%, arose from two distinct and separable sources. The first was terrain-induced. Along a 994 m west–east transect (azimuth 90.1°), the designed points matched the observed tree crowns most closely where the ground elevation remained within the narrow 23–24 m band, whereas the deviations increased markedly in segments where the elevation varied between 13 and 30 m. Because the planting grid was generated on a planimetric (2-D) orthophoto without a digital elevation model, slope-induced horizontal foreshortening was not compensated, so the projected spacing departed from the true ground spacing as terrain relief increased. This component is a property of the design method and would be reduced by incorporating a DEM into the grid-generation step.

The second source was operational and unrelated to the rover's positioning accuracy. The geo-tagging analysis revealed a difference of 474 points between the designed grid and the trees actually present in the block. This gap is attributable to (i) differences in the starting reference point chosen by the field crew during the original planting, which shifted the entire lattice, and (ii) unplanted or non-plantable areas, such as drainage, roads, and natural gaps, that remained included in the digital grid. These operational factors reflect how the historical plantation was established rather than any error introduced by the rover and they inflate the apparent mismatch independently of terrain. Separating the two sources indicates that the rover's own contribution to the ±25% figure is minor; the dominant drivers are the absence of terrain correction in the design and the partial, offset implementation of the original planting. It should be noted that the ±25% value is a coarse, largely visual estimate of spatial correspondence; a more rigorous evaluation, planned for future work, would compute point-to-point nearest-neighbor distances between each designed point and its matched tree crown and report their RMSE and distribution, after DEM-based terrain correction and re-registration of the lattice to a common starting reference.

4.5 Operational Range and Scalability

The principal operational limitation of the system is the range of the LoRa correction link. Reliable delivery of RTCM messages was maintained up to about 90 m, beyond which packet loss exceeded 20% and positional error increased. Several complementary strategies can extend the usable coverage. The simplest is operational: relocating the base station closer to the active block so that the working baseline remains within the reliable range. For larger blocks, intermediate relay or repeater nodes can forward the RTCM packets and a LoRa mesh topology can provide multi-hop coverage across an entire estate. Alternatively, a master–secondary configuration with multiple coordinated base stations can blanket a wide area, with each rover selecting the nearest base. Where intermittent cellular coverage exists, a hybrid scheme that falls back to NTRIP over the mobile network can supplement the local LoRa link. Finally, the rover guidance can be integrated with semi-autonomous or robotic markers and planters, so that once corrections are available, the planting points are staked or seeded automatically, reducing operator dependence and further improving repeatability. These directions would allow the present single-base, single-rover prototype to scale toward estate-wide deployment without sacrificing its low-cost, open character.

Overall, the testing results demonstrate that the proposed system can deliver the accuracy required for practical oil palm planting-pattern implementation. The rover maintained a stable 3D Fixed / RTK Fixed status for five minutes at the benchmark point and achieved a horizontal positional error of 8.95 cm relative to the static GNSS reference. LoRa tests showed that PDR remained high at short ranges but dropped, with packet loss exceeding 20%, once the base–rover distance exceeded about 90 m. In the planting trials, the mean deviations from the designed spacing were 8.40 cm (square) and 7.78 cm (triangular), with the largest errors confined to the areas farthest from the base station, consistent with the LoRa range limitation.

5 Conclusions and Future Directions

Based on the overall testing campaign, the proposed planting-pattern determination system, integrating the ArduSimple RTK2B, LoRa communication, and orthophoto-based digital maps, meets the accuracy requirements for oil palm plantation establishment. Benchmark tests against a static GNSS reference yielded a horizontal positional error of 8.95 cm under RTK Fixed conditions, and the planting trials produced mean spacing errors of 8.40 cm (RMSE 9.28 cm) and 7.78 cm (RMSE 9.08 cm) for the square and triangular patterns, respectively, both within the 10 cm tolerance. The LoRa experiments confirmed that base–rover distance strongly affects the reliability of the correction link, with packet loss exceeding 20% beyond about 90 m and the highest spacing errors occurring in the farthest areas.

The comparison with the actual oil palm field at PT Bina Sawit Makmur (BSM) Sampoerna Agro indicated an overall correspondence of around ±25%, with a 474-point difference between the designed and existing trees. As shown above, this mismatch was driven mainly by terrain relief that was not corrected in the planimetric design and by operational factors in the original planting, rather than by the rover's positioning accuracy.

In summary, a low-cost RTK GNSS–LoRa system combined with orthophoto-based design and a smartphone navigation interface can provide practical support for precise oil palm planting-pattern implementation, offering a more accessible alternative to high-end proprietary GNSS solutions that can be adapted to other plantation crops and precision-agriculture applications. Future work will focus on extending LoRa coverage using repeaters or mesh configurations, incorporating digital elevation models into the design process, automating post-planting quality-control verification, and integrating the system with semi-autonomous markers.

References

[1] Directorate General of Plantation, *Tree Crop Estate Statistics of Indonesia 2016–2018*, Jakarta, Indonesia: Ministry of Agriculture, 2017.

[2] Latifian, M., Rahnama, A.A. & Sharifnezhad, H., *Effects of Planting Pattern on Major Date Palm Pests and Diseases Injury Severity,* Int. J. Agric. Crop Sci., 4(19), pp. 1443-1451, 2012.

[3] Agro-06/00, *Standard Operating Procedures for Oil Palm Plantation Management, SOP-Agro-06/00 Document,* pp. 1-9, 2016. (Text in Indonesian)

[4] Gumilar, R., *Analysis of the Accuracy of Land Survey Measurements Using the Real-Time Kinematic Global Navigation Satellite System,* Geoplanart, **5**(2), pp. 16–24, 2023. (Text in Indonesian)

[5] Aini, N., Aimrun, W., Amin, M.S.M., Ezrin, M.H. & Shafri, H.Z., *Auto Guided Oil Palm Planter by using Multi-GNSS,* IOP Conf. Ser. Earth Environ. Sci., **20**(1), 2014. doi: 10.1088/1755-1315/20/1/012013.

[6] Jayaselan H.A.J. & Ahmad, D., *Development of a Mechanization Selection System for Oil Palm Plantations with Alternative Planting Patterns,* J. Oil Palm Res., **23**(APRIL), pp. 990-998, 2011.

[7] Suwardhi, D., *Mapping by using UAV Photogrammetry*, LPPM ITB, 2023. https://lppm.itb.ac.id/wpcontent/uploads/sites/55/2023/11/PemetaanUAV

-FOtogrametri-Deni-Suwardhi.pdf (19 November 2025). (Text in Indonesian)

[8] Pitri, D.T., *Interpretation of Geospatial UAV Orthophoto Data for Oil Palm Plantation Monitoring.* Univ. Sumatera Utara, 2018. Available: https://repositori.usu.ac.id/handle/123456789/12171 (28 November 2025) (Text in Indonesian)

[9] Mahato, S., Goswami, M. & Bose A., *Real-time Kinematic (RTK) Position Solution Performance of Compact, Low-cost GNSS Receiver–Antenna Combinations,* Survey Review, **57**(402), pp. 301-311, 2025. doi: 10.1080/00396265.2024.2429532.

[10] Mahato, S., Goswami, M., Kundu, S.. & Bose, A., *Single Baseline Long Distance RTK using CLS GNSS Module & Open-source Software: Case Study from India,* IETE Journal of Research, **70**(3), pp. 2905-2916, 2024. doi: 10.1080/03772063.2023.2192424.

[11] Mahato, S., Goswami, M. & Bose, A., *Position Solution Quality Performance of Compact, Low-cost, Dual-frequency GNSS Modules,* in XXXVth URSI General Assembly and Scientific Symposium, Sapporo, Japan, 2023. doi: 10.46620/URSIGASS.2023.3417.GPKR5508.

[12] Mahato, S., Shaw, G., Santra, A., Dan, S., Kundu, S. & Bose, A., *Low-cost GNSS Receiver RTK Performance in Forest Environment,* in 2020 URSI Regional Conference on Radio Science, Varanasi, India, 2020. doi: 10.23919/URSIRCRS49211.2020.9113621.

[13] Famiglietti, N.A., Cecere, G., Grasso, C., Memmolo, A. & Vicari, A.*, A Test on the Potential of a Low-cost Unmanned Aerial Vehicle RTK/PPK Solution for Precision Positioning,* Sensors, **21**(11), 3882, 2021. doi: 10.3390/s21113882.

[14] GETSI, *Static GNSS Survey Methods,* Science Education Resource Center (SERC) at Carleton College, 2023. Available: https://cdn.serc.carleton.edu/files/getsi/teaching_materials/highprecision/static_gnss_survey_methods.v5.pdf (22 November 2025).

[15] M. Chwalisz et al.*, Evaluating the LoRaWAN Protocol Using a Permanent Outdoor Testbed,* 2019 IEEE Wireless Communications and Networking Conference (WCNC), Marrakech, Morocco, 2019. pp. 1-8. doi: 10.1109/WCNC.2019.8885931.